Dynamics of Glucose-Lactose Diauxic Growth in E. coli

Zhao Lu* and Michael A Lee
Department of Physics, Kent State University, Kent, OH 44240, USA

We present a mathematical model of glucose-lactose diauxic growth in *Escherichia coli* including both the positive and negative regulation mechanisms of the lactose operon as well as the inducer exclusion. To validate this model, we first calculated the time evolution of βgalactosidase for only the lactose nutrient and compared the numerical results with experimental data. Second, we compared the calculated cell biomass of the glucose-lactose diauxic growth with the experimental optical density of the diauxic growth for a particular *E. coli* MG 1655. For both cases, the numerical calculations from this model are in good agreement with these two experiments' data. The diauxic growth pattern of a wild type *E. coli* was also investigated.

I. INTRODUCTION

The complexity of how cells respond to their changing environments requires the understanding of gene regulation and protein expression. An interesting diauxic growth pattern of *Escherichia coli* (*E. coli*) on glucose and lactose nutrients has been extensively studied and well characterized for a long time (e.g., Jacob and Monod [19], Jacob and Monod [20], Beckwith [1], Nester et al. [23]). Fig. 1 illustrates a biphasic growth pattern of *E. coli* in a glucose-rich and lactose-rich medium. Since extra energy is required to make additional enzymes (lactose permease and βgalactosidase) for the lactose transportation and metabolization, the utilization of glucose was always preferred. The diauxic growth pattern can be explained by the lactose operon genetic regulatory network and the inducer exclusion.

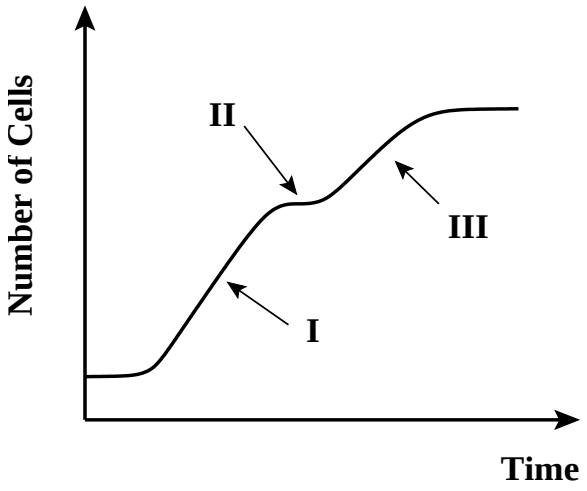

FIG. 1: Diauxic Growth of *E. coli* on glucose and lactose. I: glucose growth phase; II: lag phase; III: lactose growth phase. *E. coli* preferentially takes glucose and when the glucose nutrient is depleted, a short lag phase appears before the cell growth resuming on the lactose utilization. Note that the logarithmic scale used in the number of cells.

Quantitative mathematical models of the lactose operon and diauxic growth have been investigated by many authors (Jong [8], Yagil and Yagil [32], Wong et al. [31], Kremling and Gilles [11], Kremling et al. [12], Mahaffy and Savev [18], Yildirim and Mackey [33], Satillan and Mackey [28], Bailey [2], Lee and Bailey [15], Lee and Bailey [16], Laffend and Shuler [13], Ozbudak et al. [26]). A recent genetically structured model for the diauxic growth of *E. coli* on glucose and lactose was developed by Wong et al. [31]. In their work, all known information including the lactose operon transcription and translation processes, the flux models of unidirectional glucose transport and bidirectional lactose transport, the inducer exclusion, the catabolite repression, and the repressor DNA loop repression, was described by a set of nonlinear ordinary differential equations (ODEs). By solving the system ODEs with appropriate experimental parameters, they produced a typical diauxic growth curve. However, no comparison was made with experimental data. Kremling and Gilles [11] and Kremling et al. [12] developed another structured mathematical model of glucose-lactose diauxic growth and it was validated by their own experiments.

Many other studies of lactose operon modeling were on the stability analysis of steady states and dynamic evolutions of *E. coli* on the lactose nutrient only. Mahaffy and Savev [18] and Yildirim and Mackey [33] developed their mathematical models including the time delay of translation processes explicitly. Similar to Yagil and Yagil [32], a simple Hill's function was applied as the regulation function of the lactose operon. Mahaffy and Savev [18] reported that there was a hysteresis of solution within a certain range of the parameter space. Yildirim and Mackey [33] showed a bistable steady state of the lactose operon. However, a common problem in their model was the assumption of a constant growth rate. This assumption is only valid in the exponential growth period, and may not be true through the period from the initial growth of *E. coli* to the exponential balanced growth.

In this paper, we extended the mathematical model proposed by Wong et al. [31] on one hand by including more realistic complexities (for example, the time

*Corresponding author; Electronic address: zlu2@kent.edu

delay of translation processes of protein synthesis); on the other hand, we simplified their model (for example, by using an intuitive definition of the growth rate (Kremling et al. [12]). As is known, validation and prediction are two essential features for any useful mathematical model for real biological systems. Therefore, the focus of this present work is to validate this extended mathematical model by two particular experiments' data, and predict the diauxic growth pattern of a wild type *E. coli* on glucose and lactose in general.

To construct the mathematical model, we made four changes to the model of Wong et al. [31]. First, a modified bidirectional flux model based on a simple microscopic description of the symmetric lactose transport was derived. This change connects the difference of the influx and efflux of the lactose transport. Second, the time delay of translation processes was considered explicitly. As pointed out by Yildirim and Mackey [33], it was important but failed to appear in Wong's model. In addition, the rate of translation was modeled by an empirical function of the *E. coli* growth rate (Bremer and Dennis [3]). The third change concerned the growth rate of *E. coli*. In our treatment, we used the growth rate that depends on the glucose and lactose uptake rate. This intuitive definition let us eliminate the stiffness of the model of Wong et al. [31]. The last change was on the inducer exclusion. A Hill's function with a higher steepness to model the inhibition of lactose permease was employed since it was reported by Kimata et al. [9] that the inducer exclusion may play a major role in the glucose-lactose diauxic growth pattern.

The studies presented here had three parts. In the first part, we defined three levels of βgalactosidase: basal level, partly induced level, and fully induced level. For the lactose nutrient only, we calculated the time evolution of βgalactosidase and compared it to Knorre [10] experimental data. In the second part, we studied the diauxic growth of a particular *E. coli* MG 1655. The cell biomass of *E. coli* MG 1655 was calculated by inputting the same concentrations of glucose and lactose as those in experimental studies by Chang et al. [4] (http://www.ou.edu/microarray/oumcf/growth_trans.htm). To fit the experimental data, we converted the cell biomass to the corresponding experimental optical density (OD), and provided an analysis of the discrepancy between the numerical results and the observed OD in the lactose growth period. The numerical results of the mathematical model for both cases are in good agreement with these two experiments' data. In the third part, by adjusting the rate of glucose transport, the diauxic growth pattern of a wild type *E. coli* was studied.

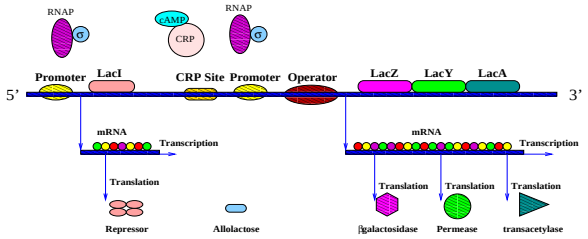

FIG. 2: The lactose operon (Nester et al. [23], Beckwith [1], Echols [5]) is a segment of DNA molecule in an *E. coli* cell with its length ∼5000 *base pairs* (*bps*). It consists of three genes and three different regulation sites. The three genes are *lacZ*, *lacY* and *lacA* and their products are βgalactosidase, lactose permease, and transacetylase respectively. The enzyme βgalactosidase breaks lactose and allolactose into glucose and galactose, and transforms lactose to allolactose. Lactose permease is in charge of transporting lactose into or out of the cell. The function of transacetylase is not clear in the lactose operon regulatory network, and thus is not considered in this study. Three different regulation sites are cyclic AMP (cAMP) receptor protein (CRP) binding site, promoter, and operator. These three binding sites provide physical locations for three transcription factors: CRP, RNA polymerase, and repressor protein. Upstream of the lactose operon, a repressor gene *lacI* constitutively expresses the repressor protein.

TABLE I: Effectors, transcription factors and binding sites in the lactose operon system

Effector	Transcription factor	Regulation site
σ	RNA polymerase	promoter
cAMP	CRP	CRP binding site
allolactose	repressor	operator

II. THE MODEL

A. Biological model

The structure of the lactose operon system is shown in Fig. 2. The transcription of the lactose operon is regulated by the interaction of three transcription factors with their corresponding effectors at their binding sites in DNA listed in Table I. The σ effector, if associated with the RNA polymerase, can help the RNA polymerase to find its promoter site and prepare to initiate the transcription.

The lactose operon genetic regulatory network has both positive and negative feedback loops. The catabolite repression is positively regulated by the extracellular glucose. The high level of the extracellular glucose results in a low level of cyclic adenosine monophosphate (cAMP), so cAMP receptor protein (CRP) is not activated. If the extracellular glucose density is very low, then a high level of cAMP will result in an activation of CRP. cAMP as a modulator binds CRP to positively control its DNA binding activation. The complex of

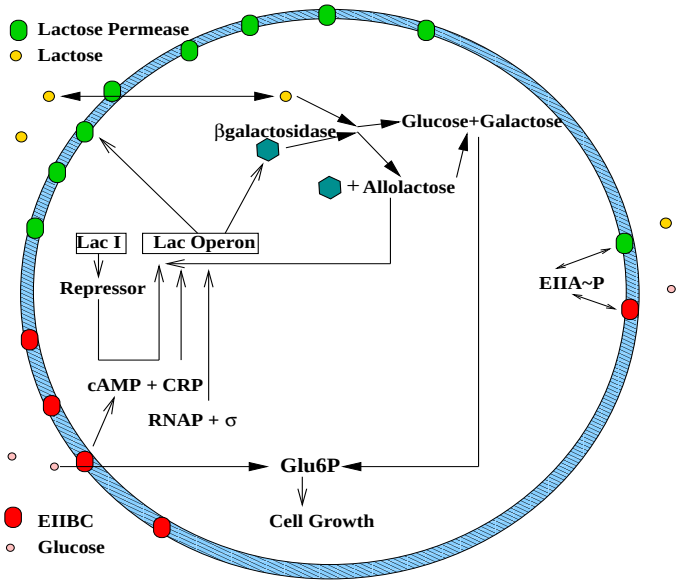

FIG. 3: The metabolic pathway of glucose-lactose diauxic growth in *E. coli*

.

cAMP∼CRP at its binding site facilitates RNA polymerase binding at the promoter site and helps RNA polymerase in the transcription of the lactose mRNA.

The negative regulation feedback loop is controlled by the interaction between the complex of repressor-operator and allolactose. If the intracellular allolactose (the nature inducer) is not available, the repressor protein is bound at the operator site tightly, and thus the transcription of RNA polymerase is blocked. If the level of the intracellular allolactose is high, the allolactose will bind with the repressor and free the operator so that the transcription of the lactose operon can be initiated. It was reported by Oehler et al. [25] that the binding affinity of the complex of repressor protein and allolactose at the operator site was lowered by about a few thousand fold. If the transcription of the lactose operon is derepressed, then βgalactosidase and lactose permease will be expressed.

The glucose-lactose diauxic growth can be explained by the positive and negative regulation feedback loops and the inducer exclusion. The mechanism of the lactose transporter protein (lactose permease) inhibited by the interaction between lactose permease and the unphosphorylated enzyme type II A subunit (EIIA), a component of phosphoenolpyruvate:sugar phosphotransferase system (PTS) (Postma et al. [27]), is called the inducer exclusion, or glucose effects. Fig. 3 illustrates the metabolic pathway of *E. coli* in a glucose and lactose medium. When the extracellular glucose is negligible, the inducer exclusion and the positive regulation are minimized. Because it takes time to induce the lactose operon to make the necessary enzymes βgalactosidase and lactose permease to transport and metabolize lactose, a plateau with a negligible growth rate shows up before the cell growth on the lactose utilization. The plateau shown in Fig. 1 characterizes the glucose-lactose diauxic growth in *E. coli*.

B. Mathematical model

The dynamics of the glucose-lactose diauxic growth has been modelled by Wong et al. [31] by using a set of nonlinear ODEs. Here, we present the four changes in the extended mathematical model which are different from the Wong et al. [31] study. The complete rate equations to solve the dynamics of the glucose-lactose diauxic growth are listed in Appendix A. The units of the intracellular quantities and the extracellular quantities are $mol/gDCW$ ($gDCW$: gram Dry Cell Weight) and M respectively. The units of the intracellular quantities can be converted to M by using the cell density $\rho_{cell} = 300\ gDCW/L$ when necessary. The unit of biomass is $gDCW$.

1. *Flux model of lactose transport*

The flux of the lactose transport entering the cell is given by,

$$\frac{d\rho^o_{lac}(t)}{dt} = -k^t_{lac}(\rho_{cell}\rho_{perm}(t))\frac{\rho^o_{lac}(t) - \rho_{cell}\rho^i_{lac}}{\rho^o_{lac}(t) + \rho_{cell}\rho^i_{lac}(t) + \rho^*_{lac}}, \quad (1)$$

where ρ^o_{lac}, ρ^i_{lac}, and ρ_{perm} denote the densities of the extracellular lactose, the intracellular lactose, and the intracellular lactose permease respectively. The rate constant of the lactose transport is k^t_{lac} and the saturation constant of lactose transport is ρ^*_{lac}. The flux of the lactose transport is proportional to the the density of lactose permease regulated by the lactose operon. The derivation of Eq. 1 based on the microscopic description is given in Appendix B.

Eq. 1 is different from the flux model of the lactose transport given by Wong et al. [31]. First, this flux model is proportional to the difference of the extracellular and intracellular lactose densities. Second, there is only one saturation constant for both influx and efflux of the lactose transport. In our numerical results shown later, the intracellular lactose density is very small compared to the extracellular lactose density. This could explain why the saturation constant of the efflux is very high in the efflux model of the lactose transport by Wong et al. [31].

2. *Time delay of translation*

Proteins such as βgalactosidase and lactose permease are synthesized in the translation process. The rate equa-

tions of them are,

$$\frac{d\rho_{\beta gal}(t)}{dt} = \frac{1}{4}k_{ts}\rho_{mRNA}(t-\tau_\beta) - (\mu + d_p)\rho_{\beta gal}(t) \quad (2)$$

$$\frac{d\rho_{perm}(t)}{dt} = k_{ts}\rho_{mRNA}(t-\tau_p) - (\mu + d_p)\rho_{perm}(t), \quad (3)$$

where ρ_{mRNA} denotes the density of mRNA molecules. τ_β and τ_p are the time delay constants of βgalactosidase and lactose permease respectively. These two constants are the results due to the finite speed of producing polypeptides at the ribosome sites. The factor $\frac{1}{4}$ in Eq. 2 accounts for a βgalactosidase molecule consisting of four monomers. The number of proteins produced per unit time, i.e., the rate of translation constant, is k_{ts}. This rate is dependent on the growth rate ([3, 16]). Here, the relationship between k_{ts} and the growth rate $\mu(t)$ was assumed to be,

$$k_{ts} = \begin{cases} k_{ts}^{eff}(\frac{\mu}{\mu_0})^{\frac{1}{m}} + k_{ts}^{basal} & \mu \le \mu_0, \\ k_{ts}^{eff} + k_{ts}^{basal} & \mu > \mu_0. \end{cases}$$

where μ_0 is the growth rate corresponding to a one-hour doubling time. If there is no lactose in the nutrient pool, then the lactose operon is maintained at its basal level by the stochastic and rare transcription. Thus, the rate of translation k_{ts} was assumed to be k_{ts}^{basal}. If lactose nutrient is available, then the rate of translation is increased until $\mu > \mu_0$. The higher the steepness parameter m is, the faster the rate of translation k_{ts} returns to its normal level from k_{ts}^{basal}. The protein degradation time of βgalactosidase and lactose permease is d_p.

3. Inducer Exclusion

When a glucose molecule is transported into a cell, it is phosphorylated into a glucose-6-phosphate by a phosphorylated EIIA. The unphosphorylated EIIA inhibits the lactose permease and thus prevents the lactose transport. This inhibition is currently known only for the extracellular lactose. Therefore, in the expression of the flux model of the lactose transport, an inhibition factor is attached to the influx of the extracellular lactose density. We used a similar Hill's function (Wong et al. [31]) but with a higher steepness for modeling the inducer exclusion process in this study. It was reported by Kimata et al. [9] that glucose effects may play an important role in the diauxic growth pattern. To incorporate this information, the inducer expression is modeled by,

$$R_{iex} = \frac{K_{iex}^2}{K_{iex}^2 + \rho_{glu}^o(t)^2}.$$

where the inhibition constant is K_{iex} and the extracellular glucose density is ρ_{glu}^o. The total flux of lactose coming into the cell with the inducer exclusion is now modified,

$$\frac{d\rho_{lac}^o(t)}{dt} = -k_{lac}^t(\rho_{cell}\rho_{perm}(t))\frac{\rho_{lac}^o(t)R_{iex} - \rho_{cell}\rho_{lac}^i}{\rho_{lac}^o(t) + \rho_{cell}\rho_{lac}^i(t) + \rho_{lac}^*}. \quad (4)$$

4. Growth Rate

The doubling time may be defined as the time needed for a cell absorbing the number of glucose molecules (N_{glu}^{cell}) to make a cell. To find this number N_{glu}^{cell}, the yield coefficient of glucose ($Y_{x/glu}$) and an average *E. coli* cell biomass were used. The doubling time is thus given as a function of the flux of glucose or lactose transport,

$$T_d = N_{glu}^{cell}/\frac{dN_{glu}}{dt},$$

and the growth rate is defined as $\mu = \frac{\ln 2}{T_d}$. The intracellular lactose and allolactose is hydrolyzed into glucose and galactose, and galactose is then converted into glucose. We simply used one lactose molecule contributing two glucose molecules. The growth rate is thus given,

$$\mu(t) = \frac{ln2}{N_{glu}^{'cell}}(k_{glu}^t\frac{\rho_{glu}^o(t)}{\rho_{glu}^o(t) + \rho_{glu}^*} + 2k_{lac}^t\rho_{\beta gal}(t)\frac{R_{iex}\rho_{lac}^o(t) - \rho_{lac}^i(t)}{\rho_{lac}^o(t) + \rho_{lac}^i(t) + \rho_{lac}^*}). \quad (5)$$

The rate of the glucose transport and the saturation constant of the glucose transport are denoted as k_{glu}^t and ρ_{glu}^* respectively. Note that the unit of $N_{glu}^{'cell}$ is now $mol/gDCW$. The expression of the growth rate shows that $\mu(t)$ depends on the extracellular glucose and lactose densities as well as the inducer exclusion. This intuitive definition of the growth rate (Kremling et al. [12]) avoids the stiffness resulting from the assumption of the growth rate depending on the level of glucose-6-phosphate and the extra burden of the lactose operon (Wong et al. [31]).

III. RESULTS

To solve the dynamics of *E. coli* growth on glucose and lactose nutrients, the rate equations in Appendix A were integrated by the fourth-order Runge-Kutta algorithm. All the parameters used in the rate equations are listed in Table II.

We first assumed the volume of the glucose or lactose nutrient pool to be infinite but their densities were kept as constants all the time during the cell growth. This corresponds to the average cell growth studies without considering the change of the extracellular glucose or lactose densities. Second, we took the volume of glucose or lactose pool as 1 l, but the extracellular glucose and lactose densities were varied with time. The dynamics of the glucose-lactose diauxic growth were then investigated. In

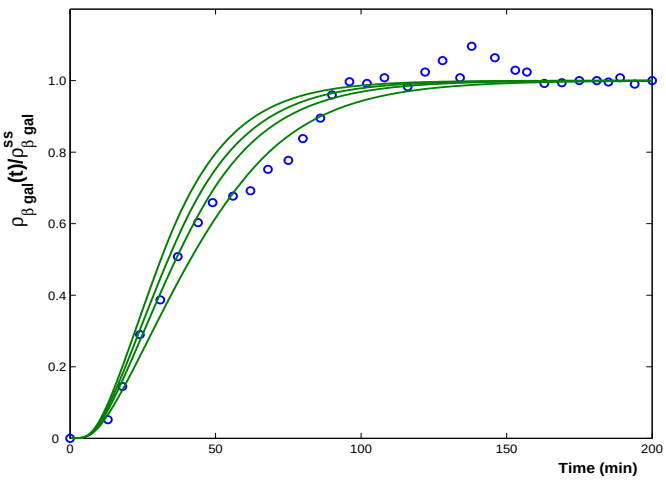

FIG. 4: Calculated curves (solid line) from the extended mathematical model, from top to bottom, $\rho^o_{lac} = 40, 4, 2, 1mM$, were compared to Knorre's experimental data (open circle).

both numerical calculations, the repressor density was assumed to be a constant, which is roughly 15 repressor proteins per cell. Finally, we studied the diauxic growth pattern of a wild type *E. coli* by adjusting the rate constant of the glucose transport.

A. Lactose growth

The induction status of the lactose operon in this study is described by the basal level, partly induced level, and fully or completely induced level. The fully induced status is defined as the maximal level of βgalactosidase when the lactose operon works at its maximal transcription efficiency. It was reported that the repression level of the lactose operon increased 2400 - 3000 fold for 10 - 15 repressor proteins per cell ([30]). Therefore, we defined the basal level of $\rho^{basal}_{\beta gal}$ as about one $2700th$ of $\rho^{max}_{\beta gal}$. The maximal value of βgalactosidase was obtained by letting the extracellular lactose density be very high. A partly induced lactose operon was defined as being between the observable induction level and the maximal induction level of βgalactosidase. Similar to Ozbudak et al. [26], this observable induction level was defined as one $100th$ of $\rho^{max}_{\beta gal}$. If the induction level of the lactose operon falls between the basal level and the observable level, the lactose operon is not induced. If the induction level is above the observable level but less than the maximal levels, then the lactose operon is partly induced.

In the numerical calculations, the maximal level of βgalactosidase, lactose permease, intracellular lactose and allolactose were obtained by letting $\rho^o_{lac} = 4 \times 10^{-2}\ M$ or above, because the maximal transcription efficiency was saturated at the very high extracellular lactose density. By using the parameters listed in Table II, $\rho^{max}_{\beta gal}$ is $2.1 \times\ 10^{-8}\ mol/gDCW$, which is about 3150 βgalactosidase molecules per cell if 1 molecule per cell corresponds to $2 \times 10^{-9}\ M$. First, we let the extracellular lactose density be zero, and solved the system ODEs. The basal level of the rate of translation k^{basal}_{ts} was adjusted and estimated such that the induction level of the lactose operon was less than or equal to the basal level. Next, a few numerical experiments were done within a range of the extracellular lactose densities from $1 \times 10^{-3}\ M$ to $4 \times 10^{-2}\ M$. The calculated results of βgalactosidase were normalized by their steady state values respectively. In Fig. 4, the numerical curves of βgalactosidase for four different levels of the extracellular lactose were plotted and compared to Knorre's experimental data ([10]). At the very beginning (less than 25 minutes) of the cell growth on lactose only, the sigmoid shape of these calculated curves can be seen in Fig. 4. This is in contrast to the hyperbolic shape given in the previous study by Satillan and Mackey [28]. The reason for this change is mainly due to the change we made on the growth rate μ, i.e., $\mu(t)$ is the time-dependent growth rate while it was assumed to be a constant in the previous study (Satillan and Mackey [28]). Other changes such as the time delay of the protein translation and the time-dependent translation rate (depending on the growth rate $\mu(t)$) also played some roles. The sigmoid shape of βgalactosidase could partly explain the lag phase of the glucose-lactose diauxic growth before the cell growth switched on lactose.

If both glucose and lactose are present in an infinite pool, then the extracellular lactose and glucose densities are to be assumed to be fixed all the time during *E. coli* growth. In this situation with the initial cell biomass or cell number assumed to be very small, bistability of the lactose operon can be studied. A numerical study of the lactose operon bistability with full consideration of interactions of regulation sites on DNA with their effectors and transcription factors has been given by Satillan and Mackey [28]. In their study, the level of βgalactosidase was taken as the order parameter to indicate the lactose operon transition from the uninduced state to the induced state. When the extracellular lactose density increased up to a threshold value, the level of $\rho_{\beta gal}$ increased discontinuously from zero to a finite value. When the process was reversed, the level of βgalactosidase decreased continuously through that threshold value.

In this study, we did the numerical calculations on both increasing and decreasing extracellular lactose density. However, we did not find discontinuation of $\rho_{\beta gal}$. A possible reason of failing to see the bistability is due to the growth rate μ. The growth rate in our study is time dependent and less than the constant growth rate used in Satillan and Mackey [28]. Moreover, the transcription efficiency of the lactose operon in their calculation was carried out by the partition function which was different from our approach. For lactose only in a nutrient pool, we found the threshold value to turn on the lactose operon at the observable induction level to be

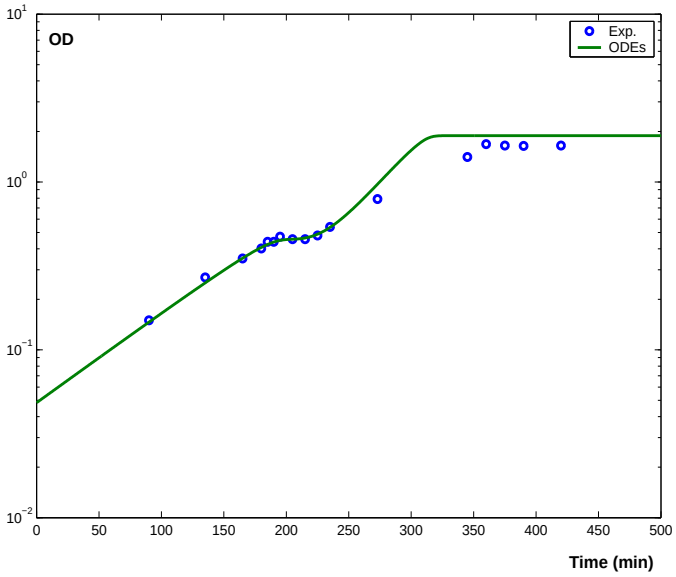

FIG. 5: Comparison of the calculated optical density (solid line) with the experimental optical density of *E. coli* MG 1655 (open circles).

$\sim$ 3.6 μM. If the extracellular lactose density is lower than this value, then the lactose operon is not induced; if the lactose density is higher than this value, then the lactose operon is partly induced. The fully induced lactose operon can only be reached by a high level of the extracellular lactose density. Ozbudak et al. [26] studied the bistability of the lactose operon when both glucose and thio-methylgalactoside (TMG) were used as substrates. The threshold value to turn on the lactose operon was estimated as 3 μM with only TMG.

B. Glucose-lactose diauxic growth

If the glucose and lactose nutrient pool is finite, then the extracellular glucose and lactose densities will be changed during the growth period of *E. coli*. There have been many experimental works on the glucose-lactose diauxic growth pattern, and most experimental data have been given in terms of OD rather than the cell biomass (e.g., [9], [4]). [4] studied the glucose-lactose diauxic growth; the experimental OD was measured at 600 nm for the *E. coli* MG 1655. The MG 1655 was cultured in 1 liter with a medium containing 0.5 g/l glucose and 1.5 g/l lactose. To monitor the cell growth, the OD at 600 nm was measured.

In numerical calculations, the glucose and lactose extracellular densities (0.5 g/l and 1.5 g/l) correspond to $\rho^o_{glu}(t = 0) = 2.78\ mM$ and $\rho^o_{lac}(t = 0) = 4.38\ mM$, respectively. It was reported that the lag phase or the transition between the glucose growth and the lactose growth lasted about 36 minutes. The OD discussed by Lawrence and Maier [14] is accurate when its values increase from 0.1 to 0.6, and is linearly related to the cell biomass. If OD is higher than 0.6, the true OD should be higher than that observed in the experimental measurement, and the linear relationship is no longer valid. The real OD can be corrected by a standard curve in a specific experiment. Since the rate of glucose uptake depends on the extracellular glucose density, the number of EIIBC, and the dwelling time associated with the phosphorylation process, different species of *E. coli* may have different numbers of EIIBC and dwelling time. This results in the different growth rate and doubling time.

The typical doubling time in glucose exponential growth of *E. coli* MG 1655 is about 60 minutes (http://www.genome.wisc.edu/resources/strains.htm). To fit the experimental data given by Chang et al. [4], the rate constant of glucose transport, k^t_{glu}, was taken as $2.1 \times 10^{-4}\ mol\ glu/gDCW/min$ while a typical range of this rate constant is 1.0 - 3.2$\times 10^{-4}\ mol\ glu/gDCW/min$. The rate constant of glucose transport determines the doubling time of the cell growth on glucose (see Eq. A1).

The calculated OD in Fig. 5 is in good agreement with the experimental OD during the glucose growth and the lag phase, but it is higher during the lactose growth. This discrepancy can be explained by the OD measurement mentioned before. Since the OD during the lactose growth is greater than 0.6, the real OD should be higher than the experimental measured OD (Lawrence and Maier [14]), and a standard calibration can be applied to correct the measurement due to the insensitivity of the light scattering. This statement actually confirms that the higher calculated curve of OD is consistent with the analysis of the real OD measurement. Because the initial cell mass given in this study is very small, $10^{-3}\ gDCW$, we have shifted the time and used a proportional constant between the cell biomass and the OD. The proportional constant between the OD and the cell biomass is 2.62, i.e, $OD = 2.62X$. In Fig. 5 the lag phase was estimated to be 32 - 38 minutes.

C. Diauxic growth pattern of a wild type E. coli

The doubling time of the typical wild type *E. coli* is usually within 20 to 40 minutes, which is lower than the doubling time of *E. coli* MG 1655. To reflect this characteristic, we increased the rate constant of glucose transport ($k^t_{glu} = 3.2 \times 10^{-4}\ mol\ glu/gDCW/min$) for a wild type *E. coli*.

In the numerical calculations, four levels of the initial extracellular glucose and lactose were set as: $\rho^o_{glu}(t = 0) = \rho^o_{lac}(t = 0) = 1,\ 2,\ 3,\ 4\ mM$. The initial levels of mRNA, βgalactosidase, and lactose permease were set to their basal levels. The biomass was initially used as $10^{-5}\ gDCW$. All other quantities were zero initially.

In Fig. 6 we plotted time courses of cell biomass, growth rate, mRNA, βgalactosidase, intracellular lactose, extracellular lactose and glucose. The diauxic growth

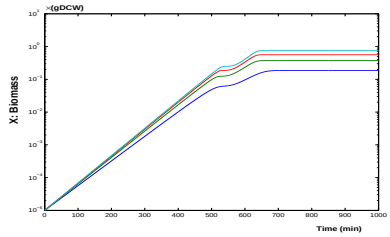

(a)Cell biomass

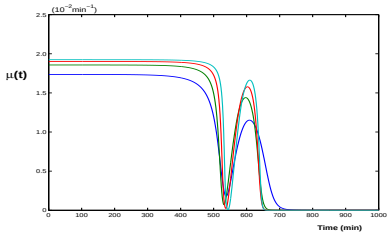

(b)Growth rate

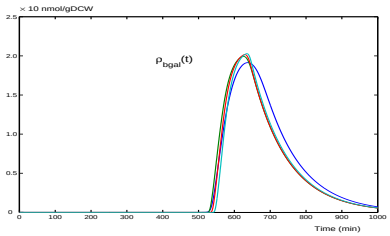

(c)βgalactosidase

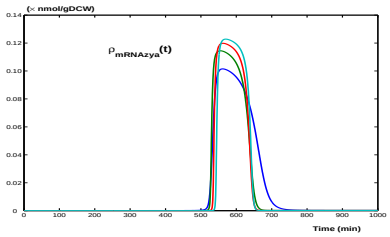

(d)mRNA$_{zya}$

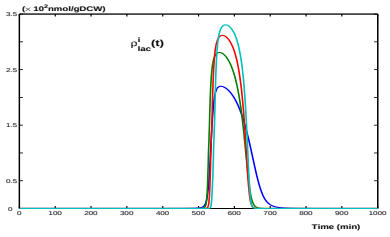

(e)Intracellular lactose

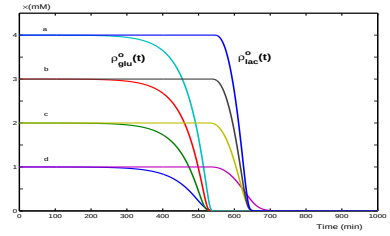

(f)Extracellular lactose and glucose

FIG. 6: Diauxic growth pattern of wild type *E. coli* with four levels of the extracellular glucose and lactose ($\rho^o_{glu}(t=0) = \rho^o_{lac}(t=0) = 1,\ 2,\ 3,\ 4\ mM$).

patterns (logarithmic scale used in the cell biomass) on glucose and lactose are shown in Fig. 6 (a). The slopes of the cell biomass represent different growth rates.

From Fig. 6 (b), during the exponential growth period of glucose, the growth rate $\mu(t)$ was almost a constant. However, when the level of the extracellular glucose decreased after 500 minutes, the growth rate $\mu(t)$ dropped rapidly. In the following lag phase, the growth rate was negligible or less than the threshold value of detecting cell growth. After the lag phase, *E. coli* restarted the lactose utilization and the growth rate increased rapidly. When the lactose nutrient was almost used up the growth rate dropped quickly again.

In Fig. 6 (b), during the lactose growth period, the growth rate $\mu(t)$ never reached a constant, so no exponential growth was reached. This is accounted for by the high cell biomass accumulated after the glucose growth period. The base cell biomass was now (5×10^{-2} - 2×10^{-1} $gDCW$. Therefore, during the lactose growth period, there were no enough lactose nutrient supplied before the lactose exponential growth was reached.

Fig. 6 (c) shows how protein βgalactosidase changed with time. The protein expression increased rapidly once the lactose utilization started. However, the βgalactosidase took a long time to decrease to zero even if there were no lactose nutrient available. This can be explained by the protein degradation time which is approximately 100 minutes. The time evolution of lactose permease was the same as βgalactosidase except at the level four times greater than the level of βgalactosidase.

The level of mRNA$_{zya}$ is shown in Fig. 6 (d). The mRNA$_{zya}$ molecules increased and decreased similar to the growth rate $\mu(t)$ during the lactose growth period. The peak densities of mRNA$_{zya}$ in Fig. 6 (d) were about 15 - 18 molecules per cell. The level of the intracellular lactose in Fig. 6 was very low and it had the same time evolution as mRNA$_{zya}$. The time courses of the extracellular glucose and lactose densities during the glucose-lactose diauxic growth are plotted in Fig. 6 (f). From this figure, the extracellular lactose was not transported into the cell before the glucose was used up, and this can be attributed to the inducer exclusion.

IV. SUMMARY

We have presented an extended mathematical model of the glucose-lactose diauxic growth in *E. coli*. The mathematical model made with four changes was validated by two experiments' data. For the lactose nutrient only in an infinite pool, the numerical result of time evolution of βgalactosidase was compared with Knorre's experimental data. For both glucose and lactose nutrients in an finite pool, the dynamics of the cell biomass were converted to the experimental OD of *E. coli* MG 1655. The discrepancy between the calculated OD and the observed experimental OD in the period of the lactose growth was analyzed. The diauxic growth pattern of a wild type of *E.*

coli was studied. The extended mathematical model in this work shows that diauxic growth patterns of different species of *E. coli* can be quantitatively investigated and understood well by integrating all available information of the involved biological processes with different time scales.

APPENDIX A: RATE EQUATIONS

The nonlinear ODEs (Wong et al. [31]) used to solve the dynamics of the diauxic growth with the four changes made in this study are:

$$\frac{d\rho^o_{glu}(t)}{dt} = -\rho_{cell}k^t_{glu}\frac{\rho^o_{glu}(t)}{\rho^o_{glu}(t)+\rho^*_{glu}}, \tag{A1}$$

$$\frac{d\rho^o_{lac}(t)}{dt} = -k^t_{lac}(\rho_{cell}\rho_{perm}(t))\frac{\rho^o_{lac}(t)R_{iex}-\rho_{cell}\rho^i_{lac}}{\rho^o_{lac}(t)+\rho_{cell}\rho^i_{lac}(t)+\rho^*_{lac}}, \tag{A2}$$

$$\frac{d\rho_{mRNA}(t)}{dt} = k_{tc}P\ \rho_{laczya}-(\mu(t)+d_{mRNA})\rho_{mRNA}(t), \tag{A3}$$

$$\frac{d\rho_{\beta gal}(t)}{dt} = \frac{1}{4}k_{ts}\rho_{mRNA}(t-\tau_\beta)-(\mu(t)+d_p)\rho_{\beta gal}(t) \tag{A4}$$

$$\frac{d\rho_{perm}(t)}{dt} = k_{ts}\rho_{mRNA}(t-\tau_p)-(\mu(t)+d_p)\rho_{perm}(t), \tag{A5}$$

$$\begin{aligned}\frac{d\rho^i_{lac}(t)}{dt} &= k^t_{lac}\rho_{perm}(t)\frac{\rho^o_{lac}(t)-\rho_{cell}\rho^i_{lac}(t)}{\rho^o_{lac}(t)+\rho_{cell}\rho^i_{lac}(t)+\rho^*_{lac}}\\ &\quad -k^{allo}_{lac}\rho_{\beta gal}(t)\frac{\rho^i_{lac}(t)}{\rho^i_{lac}(t)+K_{lac}}\\ &\quad -k^{cat}_{lac}\rho_{\beta gal}(t)\frac{\rho^i_{lac}(t)}{\rho^i_{lac}(t)+K_{lac}}-\mu\rho^i_{lac}(t),\end{aligned} \tag{A6}$$

$$\frac{d\rho_{allo}(t)}{dt} = k^{cat}_{allo}\rho_{\beta gal}(t)\frac{\rho_{allo}(t)}{\rho_{allo}(t)+K_{allo}}-\mu(t)\rho_{allo}(t), \tag{A7}$$

$$\begin{aligned}\frac{d\rho_{cAMP}(t)}{dt} &= k_{cAMP}\frac{K_{cAMP}}{K_{cAMP}+\rho^o_{glu}(t)}\\ &\quad -(k_{ex}+\mu(t))\rho_{cAMP}(t),\end{aligned} \tag{A8}$$

$$\frac{dX(t)}{dt} = \mu(t)X(t). \tag{A9}$$

Eq. A1 describes the flux of glucose transport entering the cell. The extracellular glucose density is $\rho^o_{glu}(t)$. The rate of glucose transport and the saturation constant are k^t_{glu} and ρ^*_{glu} respectively.

Eq. A2 describes the flux of lactose transport entering the cell. The extracellular lactose density is $\rho^o_{lac}(t)$, and the intracellular lactose density is $\rho^i_{lac}(t)$. The cell density ρ_{cell} is used for converting the unit $(mol/gDCW)$ of the intracellular quantities having the same unit (M) as the extracellular lactose density. The rate of lactose transport and the saturation constant are k^t_{lac} and ρ^*_{lac} respectively.

Eq. A3 describes the transcription process of the lactose operon. The densities of mRNA and the lactose genes are $\rho_{mRNA(t)}$ and ρ_{laczya}. The degradation rate and the rate of transcription are d_{mRNA} and k_{tc} respectively. The maximal transcription rate k_{tc} is estimated as $2/s$, for the size of mRNA polymerase with the σ factor is $\sim$ 37 nm and the elongation rate of mRNA molecule is about 50 bps/s.

The factor P, representing the transcription efficiency of the lactose operon, is decomposed into $P = P_1 \times P_2 \times P_3$. P_1 is the probability of the complex of RNA polymerase with the σ factor at the promoter site; P_2 is the probability of the complex cAMP and CRP at the CRP binding site; and P_3 is the probability of the empty operator site. The calculations of P_1, P_2 and P_3 are given in Appendix C.

Eqs. A4 and A5 describe the rate changes of βgalactosidase and lactose permease. The rate of translation is k_{ts} and it depends on the growth rate $\mu(t)$. The degradation rate is d_p. Time delay constants of βgalactosidase and lactose permease are τ_β and τ_p respectively.

Eqs. A6 and A7 describe the rate changes of the intracellular lactose and allolactose. The hydrolysis of lac-

tose and allolactose was assumed to follow the Michaelis-Menten mechanism. The saturation constants of the lactose and allolactose hydrolyzation are K_{lac} and K_{allo}. The rate constants of transforming lactose or allolactose to glucose and galactose are k_{lac}^{cat} and k_{allo}^{cat} respectively.

Eq. A8 describes the catabolite repression regulated by cAMP. The cAMP synthesis constant and inhibition constant are k_{cAMP} and K_{cAMP} respectively. Eq. A9 describes the dynamics of the cell biomass. The values of all parameters in the rate equations are given in Table II.

Table II inserted here.

APPENDIX B: DERIVATION OF THE FLUX MODEL OF THE LACTOSE TRANSPORT

The microscopic description of bidirectional lactose transport is similar to that of the glucose transport; however, the lactose transport is more complicated. For simplicity, we first derived the flux model of glucose transport and then the flux model of bidirectional lactose transport.

Glucose is transported by the glucose transporter enzyme type II BC (EIIBC), a component of PTS. In this study we assumed two states of EIIBC: either free or occupied. If the EIIBC subunit is occupied by a glucose molecule, then it can not accept any more glucose molecules until it is free again. The total number of EIIBC on the plasma membrane of *E. coli* is given at time t,

$$N_{tot}^{e}(t) = N_{f}^{e}(t) + N_{o}^{e}(t),$$

where numbers of free and occupied by glucose are $N_f^e(t)$ and $N_o^e(t)$ respectively. The total flux of nutrients into the cell depends on the number of free EIIBC and the extracellular glucose density,

$$J_{cell}^{o} = N_{f}^{e} K_c \rho_{glu}^{o}(t).$$

K_c is the proportional constant characterized by the nature of biochemical reactions of glucose and EIIBC. At any instant time, $N_o^e(t)$ glucose transporters are occupied by glucose molecules and if the time for a glucose molecule to be completely transported into the cell is t_s, we then expect the number of glucose molecules per unit time entering the cell to be,

$$J_{cell}^{i} = \frac{N_o^e}{t_s}$$

The time t_s for transporting a glucose molecule into cell may be associated with the phosphorylation process, and the time scale of this transportation process is $\sim ms$. Because it is very small compared to the time scale of changing the density of EIIBC, which is $\sim s$, these fluxes must be equal. This gives us the number of free EIIBC as,

$$N_{f}^{e}(t) = \frac{N_{tot}^{e}(t)}{1 + t_s K_c * \rho_{glu}^{o}(t)}.$$

The total glucose flux becomes,

$$J_{cell} = K_c \rho_{glu}^{o}(t) \frac{N_{tot}^{e}}{1 + t_s K_c \rho_{glu}^{o}(t)}.$$

If the characteristic density ρ_{glu}^{*} is defined as, $\rho_{glu}^{*} = 1/(t_s K_c)$ and $1/t_s = k_g$ is identified as the rate of the complex of EIIBC and glucose releasing the glucose molecule into the cell, then the total glucose flux coming into an average cell is,

$$J_{cell} = k_g N_{tot}^{e}(t) \frac{\rho_{glu}^{o}(t)}{\rho_{glu}^{o}(t) + \rho_{glu}^{*}}.$$

This is the flux model usually used in modeling glucose transport. The characteristic glucose density actually is the saturation constant of glucose transport through EIIBC. The equation of describing the rate of the extracellular glucose density is then,

$$\frac{d\rho_{glu}^{o}(t)}{dt} = -\rho_{cell} k_{glu}^{t} \frac{\rho_{glu}^{o}(t)}{\rho_{glu}^{o}(t) + \rho_{glu}^{*}}$$

where k_{glu}^{t} is the rate constant of the glucose transport including the contributions of all glucose transporters on the *E. coli* cell plasma membrane.

The transport of lactose is similar to the glucose transport. However, the lactose transport is bidirectional and cotransported with a proton ion through lactose permease. Here the kinetic constant in the lactose transport was assumed to include the effect caused by the electric potential across the cell plasma membrane. The lactose permease was assumed to have three states: free (f), occupied by lactose from outside the cell (oo), and occupied by lactose from inside the cell (oi). Symmetrical lactose transport was also assumed. The total number of lactose permease in average cell is given as,

$$N_{tot}^{l}(t) = N_{f}^{l}(t) + N_{oo}^{l}(t) + N_{oi}^{l}(t).$$

By using the same argument as in the glucose transport, the flux of lactose entering an average cell is now,

$$J_{cell} = k_l N_{tot}^{l}(t) \frac{\rho_{lac}^{o}(t) - \rho_{cell}\rho_{lac}^{i}}{\rho_{lac}^{o}(t) + \rho_{cell}\rho_{lac}^{i}(t) + \rho_{lac}^{*}},$$

where ρ_{lac}^{*} is the characteristic constant or saturation constant of the lactose transport.

The argument of two different time scales discussed above is in essence the equilibrium assumption of the glucose and lactose transportation at the longer time scale of changing the density of nutrient transporters. Indeed, the total number of glucose transporters is maintained at a constant number because the degradation is balanced with the expression of the glucose transporter. The number of lactose transporters is regulated by the lactose operon so that the net number of lactose permeases is gradually increasing. Although the total number of the lactose permeases is not a constant at the longer time scale of changing the density of lactose permease, it can be viewed as a constant at the shorter time scale of transporting lactose into the cell.

APPENDIX C: CALCULATION OF TRANSCRIPTION EFFICIENCY

The transcription initiated by mRNA polymerase will not start until the lactose operon is activated. The activation of the lactose operon is mainly determined by the transcription efficiency (Bailey [2]). Presently, three approaches are available. The first is to use a Hill's function as the regulation function and ignore the detailed molecular biochemical information of the lactose operon. This approach has been developed for a long time to simulate the regulation process of the lactose operon. The second approach is based on the assumption of fast equilibrium approximation; the transcription efficiency is treated as the product of three binding probabilities: the probability (P_1) of mRNA polymerase associated with σ factor binding at the promoter site; the probability (P_2) of a complex of CRP and cAMP binding at the CRP site; and the probability (P_3) of the free operator. From the mass balance law and given detailed biochemical reactions of the lactose operon, a set of nonlinear algebra equations can be constructed with all kinetic parameters from the experimental studies. The third approach is through identifying all possible states occurring in the binding sites and then giving a partition function considering the statistical mechanics with the rapid equilibrium approximation. The transcription efficiency, or the induction probability, is calculated by the states allowed for transcription to all possible states.

The last two approaches are better than the first one because the genetic structured information of the lactose operon is incorporated. Therefore an accurate description of the growth pattern based on the more detailed genotype information is expected. Nonetheless, a large set of kinetic parameters limits the application of the last two approaches for calculating the transcription efficiency. In this study, we used the second approach but only the main operator was considered. In addition, we assumed no dependence among these three processes. The total induction probability is thus,

$$P = P_1 \times P_2 \times P_3,$$

where

$$P_1 = \frac{\rho(mRNAp, \sigma, p)}{\rho(p)},$$

$$P_2 = \frac{\rho(CRP, cAMP, CRPsite)}{\rho(CRPsite)},$$

$$P_3 = \frac{\rho(o, free)}{\rho(o, tot)}.$$

Similar to Lee and Bailey [15], Laffend and Shuler [13], and Wong et al. [31], the transcription efficiency was calculated by three fractions. At any instant time, rapid equilibrium of the lactose operon was assumed. The biochemical reactions associated with this rapid equilibrium are written as,

$$\begin{aligned}
\rho_{x1} + \rho_{x2} &\overset{C_1}{\rightleftharpoons} \rho_{x1x2} \\
\rho_{x1} + \rho_{x3} &\overset{C_2}{\rightleftharpoons} \rho_{x1x3} \\
\rho_{x1} + \rho_{x4} &\overset{C_3}{\rightleftharpoons} \rho_{x14} \\
\rho_{x1x2} + \rho_{x3} &\overset{C_4}{\rightleftharpoons} \rho_{x1x2x3} \\
\rho_{x1x2} + \rho_{x4} &\overset{C_5}{\rightleftharpoons} \rho_{x1x2x4}.
\end{aligned}$$

The equilibrium constants C_1, C_2, C_3, C_4, and C_5 are listed in Table III. The x_1, x_2, and x_3 are transcription factor, effector, and response element respectively (see Table I). x_4 stands for the nonspecific DNA sites in *E. coli*. If the mass balance law is implied at any time, we have the following equations,

$$\begin{aligned}
\rho_{x1}(tot) &= \rho_{x1} + \rho_{x1x2} + \rho_{x1x3} + \rho_{x1x4} + \rho_{x1x2x3} + \rho_{x1x2x4} \\
\rho_{x2}(tot) &= \rho_{x2} + \rho_{x1x2} + \rho_{x1x2x3} + \rho_{x1x2x4} \\
\rho_{x3}(tot) &= \rho_{x3} + \rho_{x1x3} + \rho_{x1x2x3} \\
\rho_{x4}(tot) &= \rho_{x4} + \rho_{x1x4} + \rho_{x1x2x4}.
\end{aligned}$$

Since the number of nonspecific sites of DNA is much greater than that of regulation sites, ρ_{x4} is approximated as the total number of DNA sites, $\rho_{x4}(tot) = \rho_{tot}^{non}$. The combinations of x_1, x_2, x_3, x_4 represent the complexes of them. In this study, only complexes like x_1x_2, x_1x_3, x_1x_4, $x_1x_2x_3$, and $x_1x_2x_4$ exist.

Table III inserted here.

By using equilibrium relationships, $\rho_{x1x2} = C_1\rho_{x1}\rho_{x2}$, $\rho_{x1x3} = C_2\rho_{x1}\rho_{x3}$, $\rho_{x1x4} = C_3\rho_{x1}\rho_{x4}$, $\rho_{x1x2x3} = C_4\rho_{x1x2}\rho_{x3}$, and $\rho_{x1x2x4} = C_5\rho_{x1x2}\rho_{x4}$, three nonlinear algebraic equations with three unknown quantities, ρ_{x1}, ρ_{x2}, and ρ_{x3} are given,

$$\begin{aligned}
\rho_{x1}(tot) &= \rho_{x1} + C_1\rho_{x1}\rho_{x2} + C_2\rho_{x1}\rho_{x3} + C_3\rho_{x1}\rho_{x4} \\
&\quad + C_4C_1\rho_{x1}\rho_{x2}\rho_{x3} + C_5C_1\rho_{x1}\rho_{x2}\rho_{x4} \\
\rho_{x2}(tot) &= \rho_{x2} + C_1\rho_{x1}\rho_{x2} + C_4C_1\rho_{x1}\rho_{x2}\rho_{x3} \\
&\quad + C_5C_1\rho_{x1}\rho_{x2}\rho_{x4} \\
\rho_{x3}(tot) &= \rho_{x3} + C_2\rho_{x1}\rho_{x3} + C_4C_1\rho_{x1}\rho_{x2}\rho_{x3}
\end{aligned}$$

The $\rho_{x1}(tot)$, $\rho_{x2}(tot)$, and $\rho_{x3}(tot)$ are input densities, which can be constant values (see table II), or predicted by the differential equations [13], whereas ρ_{x1}, ρ_{x2}, and ρ_{x3} are free parts of them. The transcription efficiency $P = P_1 \times P_2 \times P_3$ can be calculated by solving three sets of the above three nonlinear algebra equations respectively. For P_1, $\rho_{x_1} = \rho_{tot}^{rnap}$, $\rho_{x_2} = \rho_{tot}^{\sigma}$, and $\rho_{x_3} = \rho_{tot}^{p}$; for P_2, $\rho_{x_1} = \rho_{tot}^{crp}$, $\rho_{x_2} = \rho_{cAMP}(t)$, and $\rho_{x_3} = \rho_{tot}^{crpsite}$; for P_3, $\rho_{x_1} = \rho_{repressor}$, $\rho_{x_2} = \rho_{allo}(t)$, and $\rho_{x_3} = \rho_{tot}^{o}$. The densities of cAMP and the intracellular allolactose are provided by the nonlinear ordinary differential equations in Appendix A.

[1] Beckwith, J., 1987. The lactose operon. In *Escherichia coli* and *Salmonella*: Cellular and Molecular Biology. Neidhardt, F.C., Ingraham, J.L., Low, K.B., Magasanik, B., and Umbarger, H.E., editors. American Society for Microbiology, Washington, DC. 1444-1452, Vol. 2.

[2] Bailey, J.E., 1986. Fundamental Biochemical Engineering. McGraw-Hill Science/Engineering/Math, 2nd edition.

[3] Bremer, H., Dennis, P., 1996. Modulation of Chemical Composition and Other Parameters of the Cell by Growth Rate. In *Escherichia coli* and *Salmonella* Thyphymurium: Cellular and Molecular Biology, Vol. 2.. Neidhardt, F.C., Ingraham, J.L., Low, K.B., Magasanik, B., and Umbarger, H.E., editors. American Society for Microbiology, Washington, DC. 1553-1569.

[4] Chang, D., Smalley, D., Conway, T., 2002. Gene Expression Profiling of *Escherichia coli* Growth Transitions: an Expanded Stringent Response Model. Molecular Microbiology, Vol. 45, No. 2, 289-306.

[5] Echols, H., 2001. Operators and promoters: The story of Molecular Biology and Its Creators. University of California Press, 1st edition.

[6] Epstein, W., Rothman-Denes, L., Hesse. J., 1975. Adenoside 3,5'-cyclic monophoshate as mediator of catabolite repression in *Escherichia coli*. Proc. Natl. Acad. Sci. USA, 72, 2300-2304.

[7] Fraser, A., Yamazaki, H., 1979. Effect of carbon sources on the rates of cyclic AMP synthesis, excretion, and degradation, and the ability to produce βgalactosidase in *Escherichia coli*. Can. J. Biochem., 57, 1073-1079.

[8] Jong, H.D., 2002. Modeling and Simulation of Genetic Regulatory Systems: A Literature Review, J. Comp. Bio., 9, No. 1, 67-103.

[9] Kimata, K., Takahashi, H., Inada, T., Postma P., Aiba, H., 1997. cAMP receptor protein-cAMP plays a crucial role in glucose-lactose diauxie by activating the major glucose transporter gene in *Escherichia coli*. Proc. Natl. Acad. Sci. USA, vol. 94, 12914-12919.

[10] Knorre, W., 1968. Oscillation of the Rate of Synthesis of βgalactosidase in *Escherichia coli* ML 30 and ML 308. Biochem. Biophys. Res. Commun. 30, 1248-1290.

[11] Kremling, A., Gilles, E.D., 2001. The Organization of Metabolic Reaction Networks II. Signal Processing in Hierarchical Structured Functional Units. Metabolic Engineering 3, 138-150.

[12] Kremling, A., Bettnbrock, K., Laube, B., Jahreis, K., Lengleler, J., Gilles, E.D., 2001. The Organization of Metabolic Reaction Networks III. Application for Diauxic Growth on Glucose and Lactose. Metabolic Engineering, 3, 362-379.

[13] L. Laffend, M. L. Shuler, 1994. Structured Model of Genetic Control via the Lac Promoter in *Escherichia coli*. Biotechnol. Bioeng., 43, 399-410.

[14] Lawrence, J., Maier, J., 1977. Correction for the Inherent Error in Optical Density Readings. Appl. Envi. Micro. Vol. 33, 482-484.

[15] Lee, S.B., Bailey, J.E., 1984. Genetically Structured Models for Lac Promoter Operator Function in the *Escherichia coli* Chromosome and in Multicopy Plasmids: Lac Operator Function. Biotechnol. Bioeng. 26, 1372-1382.

[16] Lee, S.B., Bailey, J.E., 1984. Analysis of Growth Rate Effects on Productivity of Recombinant *Escherichia coli* Population Using Molecular Mechanism Models. Biotechnol. Bioeng., Vol. 26, 66-73.

[17] Lolkema, J., Carrasco, N., Kaback, H., 1991. Kinetic analysis of lactose exchange in proteoliposomes reconstituted with purified lac permease. Biochemistry, 30, 1284-1290.

[18] Mahaffy, J., Savev, E., 1999. Stability Analysis for a Mathematical Model of the lac Operon. Quar. Appl. Math., Vol. 57, No. 1, 37-53.

[19] Jacob, F., Monod, J., 1961. Genetic Regulatory Systems Mechanisms in the Synthesis of Proteins. J. Mol. Biol., 3, 318-356.

[20] Jacob, F., Monod, J., 1961. On the Regulation of Gene Activity, Cold Spring Harbor Symp. Quant. Biol., 26, 193-209.

[21] Martinez-Bilbao, M., Holdsworth, R., Edwards, L., Huber, R., 1991. A highly reactive βgalactosidase resulting from a substitution of an aspartic acid for Gly-794. J. Biol. Chem., 266, 4979-4986.

[22] Neijssel, O., Hardy, G., Lansbergen J., Tempest, D., O'Brien, R., 1980. Influence of growth environment on the phosphoenolpyruvate:glucose phosphotransferase activities of *Escherichia coli* and Klebsiella aerogenes: A comparative study. Arch. Microbiol. 16, 121-129.

[23] Nester, E. W., Anderson, D.G., Pearsall, N.N., Roberts, C.E., Nester, M.T., 2000. Microbiology, ch7., Mcgraw-Hill College, 2nd edition.

[24] Notely, L., Ferenci, T., 1995. Differential expression of mal genes under cAMP and endogenous inducer control in nutrient-stressed *Escherichia coli*. Mol. Microbiol., 16, 121-129.

[25] Oehler, S., Amouyal, M., Kolkhof, P., Wilcken-Bergmann B., Muller-Hill, B., 1994. Quality and Position of the Three Operators of *E. coli* Define Efficiency of Repression. EMBO, vol. 13, No. 14, 3348-3355.

[26] Ozbudak, E., Thattai, M., Lim, H., Shraiman, B., Oudenaarden, A., 2004. Multistability in the lactose utilization network of *Escherichia coli*. Nature, Vol. 427, No.19, 737-740.

[27] Postma, P., Lengeler, J., Jacobson, G., 1996. Phosphoenolpyruvate-carbohydrate phosphotransferase systems. In *Escherichia coli* and *Salmonella* Thyphymurium: Cellular and Molecular Biology, Vol. 2. Neidhardt, F.C., Ingraham, J.L., Low, K.B., Magasanik, B., and Umbarger, H.E., editors. American Society for Microbiology, Washington, DC. 1149-1174.

[28] Santillan, M., Mackey, M., 2004. Influence of Catabolite Repression and Inducer Exclusion on the Bistable Behavior of the Lac Operon. Biophys. J., Vol. 86, 1282-1292.

[29] Tyson, J., Mackey, M., 2001. Molecular, Metabolic and Genetical Control: An Introduction. Chaos, Vol. 11, No1, 81.

[30] Vilar, J., Leibler, S., 2003. DNA looping and Physical Constraints on Transcription Regulation. J. Mol. Biol., 331, 981-989.

[31] Wong, P., et. al., 1997. Mathematical Models of the lac operon: Inducer exclusion, Catabolite Repression, and Diauxic growth on Glucose and Lactose. Biotechnol. Prog. 13, 132-143.

[32] Yagil, G., Yagil, E., 1971. On the Relation Between Effector Concentration and the Rate of Induced Enzyme Synthesis. Biophys. J. Vol. 11, 11-27.

[33] Yildirim, N., Mackey, M., 2003. Feedback Regulation in the Lactose Operon: A Mathematical Modeling Study and Comparison with Experimental Data. Biophys. J., Vol. 84, 2841-2851.

TABLE II: Parameters used in modeling *E. coli* growth.

Parameters	Values	References
k^t_{glu}	1.0 - 3.2 $\times 10^{-4}$ $mol\ glu/(gDCW \dot{m}in)$	[22]
ρ^*_{glu}	15 μM	[27]
k^t_{lac}	2148 min^{-1}	[31]
ρ^*_{lac}	2.6×10^{-4} M	[17]
k_{tc}	120 min^{-1}	estimated
d_{mRNA}	0.693 min^{-1}	[16]
k^{eff}_{ts}	18.8 min^{-1}	[16]
τ_β	0.05 min	[33]
τ_p	1.05 min	[33]
d_p	0.01 min^{-1}	[15]
k^{basal}_{ts}	1.8 min^{-1}	estimated
K_{lac}	1.4×10^{-4} M	[31]
K_{allo}	2.8×10^{-4} M	[31]
k^{cat}_{lac}	9540 min^{-1}	[31]
k^{allo}_{lac}	8460 min^{-1}	[31]
k^{cat}_{allo}	1.8×10^{-4} min^{-1}	[21]
K_{iex}	2×10^{-5} M	[12]
k_{cAMP}	1×10^{-5} M/min	[7]
K_{cAMP}	4×10^{-4} M	[24]
k_{ex}	2.1 min^{-1}	[6]
$Y_{x/glu}$	90 $gDCW/(mol\ glu)$	estimated
ρ_{cell}	300 $gDCW/L$	[31]
ρ_{laczya}	8.47×10^{-12} $mol/gDCW$	[31]
ρ^p_{tot}	8.47×10^{-10} $mol/gDCW$	estimated
ρ^{rnap}_{tot}	5×10^{-6} M	[31]
ρ^{σ}_{tot}	1×10^{-6} M	[31]
ρ^{crp}_{tot}	2×10^{-6} M	[31]
$\rho^{crpsite}_{tot}$	8.47×10^{-12} $mol/gDCW$	[31]
ρ^{o}_{tot}	8.47×10^{-12} $mol/gDCW$	[31]
ρ^{non}_{tot}	0.0118 M	[31]

TABLE III: Equilibrium constants involved in the biochemical reactions of *lac* operon regulation sites ([31], [15]).

Parameters	RNAP(x_1)	CRP(x_1)	Repressor(x_1)
	$\sigma(x_2)$	cAMP(x_2)	Allolactose (x_2)
	Promoter(x_3)	CRP site (x_3)	Operator(x_3)
C_1	2×10^9 M^{-1}	1×10^3 M^{-1}	2×10^6 M^{-1}
C_2	1×10^6 M^{-1}	1.1×10^5 M^{-1}	1×10^{13} M^{-1}
C_3	1×10^6 M^{-1}	5×10^3 M^{-1}	1×10^4 M^{-1}
C_4	1×10^9 M^{-1}	1×10^{10} M^{-1}	1×10^{10} M^{-1}
C_5	1×10^5 M^{-1}	1×10^5 M^{-1}	1×10^5 M^{-1}